14th Australasian Fluid Mechanics Conference
Adelaide University, Adelaide, Australia
10-14 December 2001

Mathematical Modelling of Magnetic Flow Control in a Single Belt Caster

Seyedein[1], S. H. and Aboutalebi[1], M. R.

1. Department of Materials and Metallurgical Engineering
Iran University of Science and Technology
Narmak, Tehran, 16844, Iran

Abstract

Near-net shape casting has been the subject of so many researches during the past decades where the major ones dealt with strip casting processes. One of the distinguished techniques developed in early 80's, is the single belt strip casting process in which liquid metal is introduced onto a moving water-cooled belt. The most important aspect of this process which has a crucial effect on product quality, is metal delivery system. The main point in this regard is to get the melt run out evenly onto the conveyor belt at the correct thickness, which can be handled by flow control from feeding system.

In the present work, a DC magnetic brake was considered to be used to control the flow in the downstream of the mold. This study presents some numerical results obtained from mathematical modeling of a typical single belt caster. The coupled turbulent flow and heat transfer as well as magnetic field effects were considered in this model. A low-Re $k-\varepsilon$ turbulent model was used to account for the turbulent effects. The transport equations were solved using finite volume method on a staggered grid domain. Parametric studies were performed in this study to evaluate the effect of casting conditions and magnetic field intensity on fluid flow and temperature fields.

1. Introduction

The idea of direct steel strip casting dates back to the work of Sir Henry Bessemer who tried to make the iron sheet directly from molten iron. From that time, so many researches have been carried out to develop the strip casting system on a commercial scale. Aiming at this target, various techniques including roll and belt casting processes have been devised in different countries. The main advantages of these processes over the conventional continuous casting could be energy savings and improvement of process efficiency due to shortening the production process. However, the strip casting methods are suffering from such disadvantages as lower productivity and surface quality comparing to conventional slab casting together with rolling process. The only current strip casting process under investigation that has the potential of matching the conventional casters in terms of productivity and surface quality is the single belt casting system to produce a steel strand with the thickness of about 10 mm [1,2]. On the basis of the potential merits for single belt caster, the researches have been focused on this process at Clausthal, in Germany, MEFOS in Sweden, BHP in Australia, and McGill university in Canada [1,2,3,4]. It has been recognized that the molten metal delivery system in this process can play a major role on the efficiency of the strip caster. The researchers at McGill proposed a liquid metal delivery system in which a flow control device (porous refractory filter) was used to slow down the liquid velocity normal to the water-cooled belt. Numerous mathematical and physical modeling studies were performed for this type of liquid delivery system to examine the fluid flow, heat transfer and solidification in the horizontal belt casting process [4,5,6,7].

In this paper, a three dimensional mathematical model was developed to simulate turbulent flow in the metal delivery system proposed by Guthrie s research group at McGill in which a novel magnetic flow control was adopted. In order to consider the turbulence effects, the low-Reynold two-equation $k-\varepsilon$ model of Launder and Sharma [8] was used. Various magnetic field conditions were considered in this model to evaluate the effects of magnetic field on fluid flow pattern within the computational domain. The influence of magnetic field intensity and its configurations on heat transferred to the chilled substrate was also examined.

2. Mathematical Formulation

2.1. Problem Statement and Governing Equations

The physical system to be considered in this work is a liquid metal delivery system for a single belt caster as depicted schematically in Figure 1. The molten steel is fed into a reservoir consisting of a continuous moving chilled belt and the steel strand is continuously withdrawn at substrate speed. In order to control the flow in the reservoir, various configurations of DC magnetic field were assumed as shown schematically in Figure 2. Geometrical parameters, liquid steel properties, and simulation conditions are given in Table 1.

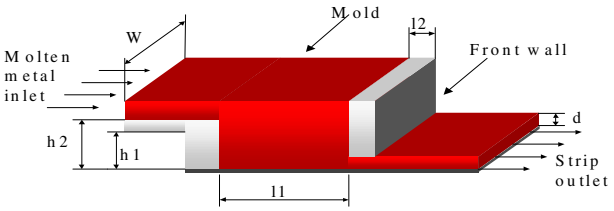

Fig 1. Schematic of strip casting system.

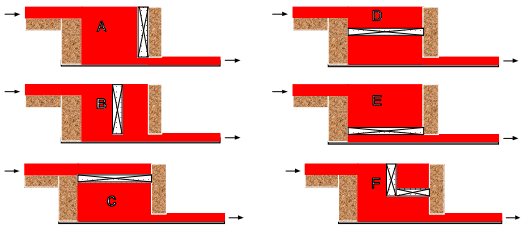

Fig. 2. Various configurations of magnetic devices adopted for the model.

Variable	Quantities	Variable	Quantities
thermal conductivity	$31\ Wm^{-1}K^{-1}$	viscosity	$0.007\ kgm^{-1}s^{-1}$
specific heat	$700\ Jkg^{-1}K^{-1}$	density	$7000\ kgm^{-3}$
magnetic flux density	0.1-1 *Tesla*	electrical conductivity	$7.19\times10^{5}\ kg^{-1}m^{-3}q^{2}s$
inlet temperature	$1480^{\circ}C$	liquidus temperature	$1454^{\circ}C$
reservoir width (*w*)	$0.2\ m$	substrate velocity	$1.8\ ms^{-1}$
back wall height (*h1*)	$0.052\ m$	reservoir height (*h2*)	$0.07\ m$
front wall thickness (*l2*)	$0.029\ m$	reservoir length (*l1*)	$0.1\ m$
strand thickness (*d*)	$0.01\ m$		

Table 1. Thermophysical properties of steel, electromagnetic conditions and geometrical parameters used for the simulation.

The major assumptions adopted in the mathematical model are:

a) Fluid is considered to be Newtonian and incompressible.
b) Three dimensional steady state flow is assumed.
c) A low-Reynolds number $k-\varepsilon$ model is employed for turbulence modeling.
d) Thermophysical properties of liquid steel are considered to be constant.
e) No slip condition at the solid surfaces is assumed.
f) Surface tension effects are not considered in the model.
g) The induced magnetic field is negligible compared to the imposed magnetic field.
h) Electromagnetic characteristics of the melt are assumed to be uniform and isotropic.

Under the above assumptions the governing equations are derived from the conservation of mass, momentum, and energy for 3-D steady state flow in Cartesian coordinates. The resulted transport equations governing the system can be represented by the following general non-dimensional partial differential equation:

$$\frac{\partial(U_i\Phi^*)}{\partial X_i}=\frac{\partial}{\partial X_i}(\Gamma_\Phi^*\frac{\partial\Phi^*}{\partial X_i})+S_\Phi^* \qquad i=1,\ 2,\ 3 \qquad (1)$$

The value of Φ^* and associated value of Γ_Φ^* for all transport equations as well as the empirical constants for turbulent model are given in Table 2.

Equation	Φ^*	Γ_Φ^*	S_Φ^*
Continuity	1	0	0
U-momentum	U	$\frac{1}{Re}\left(1+\mu_t^*\right)$	$-\frac{\partial P^*}{\partial X}+\frac{\partial}{\partial X_i}\left(\Gamma_\Phi^*\frac{\partial U_i}{\partial X}\right)+N\left(J_y^*B_z^*-J_z^*B_y^*\right)$
V-momentum	V	$\frac{1}{Re}\left(1+\mu_t^*\right)$	$-\frac{\partial P^*}{\partial Y}+\frac{\partial}{\partial X_i}\left(\Gamma_\Phi^*\frac{\partial U_i}{\partial Y}\right)+N\left(J_z^*B_x^*-J_x^*B_z^*\right)$
W-momentum	W	$\frac{1}{Re}\left(1+\mu_t^*\right)$	$-\frac{\partial P^*}{\partial Z}+\frac{\partial}{\partial X_i}\left(\Gamma_\Phi^*\frac{\partial U_i}{\partial Z}\right)+N\left(J_x^*B_y^*-J_y^*B_x^*\right)$
Kinetic energy	k^*	$\frac{1}{Re}\left(1+\frac{\mu_t^*}{\sigma_k}\right)$	$\frac{G^*}{Re}-\varepsilon^*+\frac{D_k^*}{Re}$
Rate of energy Dissipation	ε^*	$\frac{1}{Re}\left(1+\frac{\mu_t^*}{\sigma_\varepsilon}\right)$	$\frac{1}{Re}f_1C_1G^*\frac{\varepsilon^*}{k^*}-C_2f_2\frac{\varepsilon^{*2}}{k^*}+\frac{E_\varepsilon^*}{Re^2}$
Energy	h^*	$\frac{1}{Re}\left(\frac{1}{Pr}+\frac{\mu_t^*}{\sigma_t}\right)$	$N\frac{u_{in}}{\Delta H_f}\mathfrak{I}^{*2}$
Electrical potential	φ^*	1	$div\left(\mathbf{V}\times\mathbf{B}\right)$

where:

$$G^*=\mu_t^*\left(\frac{\partial U_i}{\partial X_j}+\frac{\partial U_j}{\partial X_i}\right)\frac{\partial U_i}{\partial X_j},\quad E_\varepsilon^*=2\mu_t^*\left(\frac{\partial^2U_i}{\partial X_j\partial X_k}\right)\left(\frac{\partial^2U_i}{\partial X_j\partial X_k}\right),\quad Re_t=Re\frac{k^{*2}}{\varepsilon^*},\quad f_\mu^*=e^{\frac{-3.4}{(1+Re_t^*/50)^2}},\quad \mu_t^*=Re\,C_\mu f_\mu^*\frac{k^{*2}}{\varepsilon^*},$$

$$D_k^*=2\frac{\partial\sqrt{k^*}}{\partial X_i}\frac{\partial\sqrt{k^*}}{\partial X_i},\quad N=\frac{\sigma B_0^2D}{\rho u_{in}},\quad \mathbf{J}^*=-\nabla^*\varphi^*+\mathbf{U}\times\mathbf{B}^*,\quad f_1=1,\quad f_2=1-0.3e^{-Re_t^2},\quad C_\mu=0.09,\quad C_1=1.44,$$

$$C_2=1.92,\quad \sigma_k=1.0,\quad \sigma_\varepsilon=1.3,\quad \sigma_t=0.9$$

Table 2. Summary of the non-dimensional governing equations.

The following dimensionless parameters were used to non-dimensionalize the equations.

$$X=\frac{x}{d},\quad Y=\frac{y}{d},\quad Z=\frac{z}{d},\quad U=\frac{u}{u_{in}},\quad V=\frac{v}{u_{in}},$$

$$W=\frac{w}{u_{in}}\qquad P^*=\frac{P}{\rho_\circ u_{in}^2},\quad k^*=\frac{k}{u_{in}^2},$$

$$\varepsilon^*=\frac{\varepsilon D}{u_{in}^3},\quad h^*=\frac{h}{\Delta H_f},\quad \mu_t^*=\frac{\mu_t}{\mu},\quad \mathbf{B}^*=\frac{\mathbf{B}}{\overline{\mathbf{B}}_0},$$

$$\mathbf{J}^*=\frac{\mathbf{J}}{\sigma u_{in}\overline{\mathbf{B}}_0},\quad \varphi^*=\frac{\varphi}{u_{in}\overline{\mathbf{B}}_0 D} \qquad (2)$$

where, d is strip thickness, u_{in} is inlet velocity, h is sensible heat and ΔH_f is the latent heat of fusion of steel.

2.2 Boundary Conditions

The schematic of the caster representing the computational domain adopted in this work is shown in Fig. 1. Because of symmetry, the transport equations have been solved for the half of the domain. The following boundary conditions were applied in this simulation:

Inlet boundary condition:

The uniform profile for all variables were used at the inlet surface as follows:

$$U=U_{in},\quad V=W=0,\quad h=h_{in},\quad k=0.01,$$

$$\varepsilon=c_\mu(0.01)^{3/2}/0.05,\quad \frac{\partial\varphi}{\partial X}=0$$

It is noted that the value of k and ε were selected from semi-empirical equations presented by Lai et al. [9].

Free surface :

The normal gradient of all variables were set to zero except the velocity perpendicular to the surface which itself was assumed to be zero.

$$\frac{\partial U}{\partial Y}=\frac{\partial W}{\partial Y}=\frac{\partial k}{\partial Y}=\frac{\partial \varepsilon}{\partial Y}=\frac{\partial h}{\partial Y}=\frac{\partial \varphi}{\partial Y}=0 \qquad V=0$$

Symmetry plane :

The same boundary conditions as those of free surface, were used here.

$$\frac{\partial U}{\partial Z}=\frac{\partial V}{\partial Z}=\frac{\partial k}{\partial Z}=\frac{\partial \varepsilon}{\partial Z}=\frac{\partial h}{\partial Z}=0 \qquad W=\varphi=0$$

outlet :

Fully developed conditions were adopted at the outlet, i.e., axial gradients of all dependent variables were assumed to be zero.

$$\frac{\partial U}{\partial X}=\frac{\partial V}{\partial X}=\frac{\partial W}{\partial X}=\frac{\partial k}{\partial X}=\frac{\partial \varepsilon}{\partial X}=\frac{\partial h}{\partial X}=\frac{\partial \varphi}{\partial X}=0$$

Moving surface :

Assuming no slip condition at the moving belt, the velocity in the direction of movement will be equal to the belt velocity and the two others as well as k and ε are set to zero. In terms of temperature at moving substrate a constant liquidus temperature is considered.

Walls of reservoir:

With the assumption of no slip on the solid walls, velocities plus k and ε are set to zero and for temperature an adiabatic condition is assumed

3.Numerical Solution Methodology

The governing equations (Eq. 1) associated with the boundary conditions were solved numerically using the control-volume based finite difference method. The hybrid-scheme, which is a combination of the central difference scheme and the upwind scheme, was used to discretize the convection terms. A staggered grid system, in which the velocity components are stored midway between the scalar storage locations, was used. In order to couple the velocity field and pressure in the momentum equations, the well known SIMPLE-algorithm suggested by Patankar [10] was adopted. The computer code developed in this study is basically similar to the code already developed by the authors where was successfully used to simulate the electromagnetic brake in slab continuous casters [11]. The Computations were carried out over $30\times25\times15$ and $40\times30\times20$ grids for X, Y, and Z-direction respectively. As predicted results remained unchanged by refining the grid size and for the sake of computational economy, a $30\times25\times15$ grid size were selected for all of the numerical simulations reported here. The grid points closest to the solid wall were very carefully employed such that they lie within the laminar sub-layer as required by the low-Re $k-\varepsilon$ turbulence model.

4.Computed results and discussion

The delivery of liquid steel onto the cooling substrate should be controlled in such a manner that the normal velocity to the belt at outlet to be so small that prevents from remelting the solid layer. In the present computational study, various DC magnetic brake configurations were used to control the fluid flow in the reservoir of the single belt caster. Figure 3 represents the effect of magnetic flux density on the velocity field for type-A magnetic device.

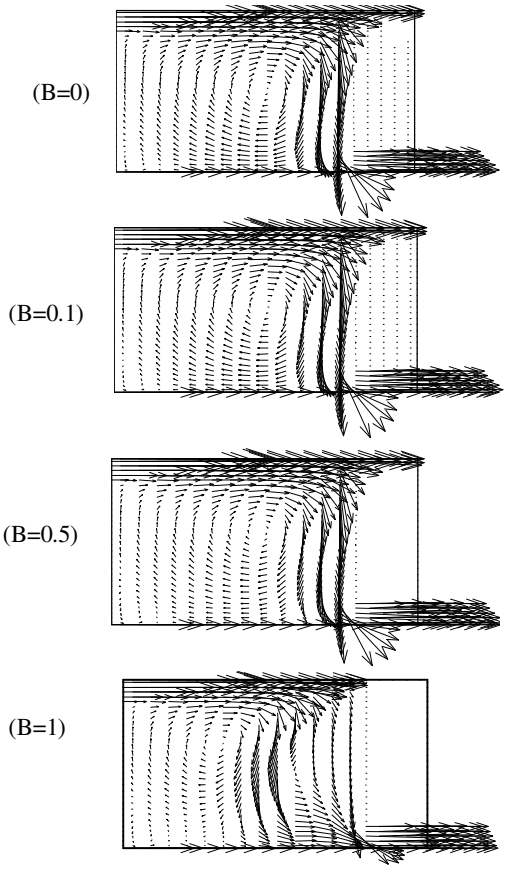

Fig. 3. The effect of magnetic flux density on the velocity field (type-A).

As can be seen from this figure, in the case of no magnetic field the impinging flow on the substrate and backward velocity are so high that could be resulted in remelting the solidified shell. By increasing the flux density, the recirculation zone is shifted towards the back wall and the impinging flow intensity over the substrate is suppressed.

Figure 4 shows the effect of magnetic field configurations on flow pattern in the reservoir. For this purpose six different types as depicted in figure 2 were studied. For all types the magnetic flux density was assumed to be constant ($B = 1\ T$). The comparison of velocity field for these types reveals that the vertical types can result in a better flow control at the substrate close to the outlet. The most suppression of normal velocity to the substrate can be achieved by the combination of vertical and horizontal types (type-F).

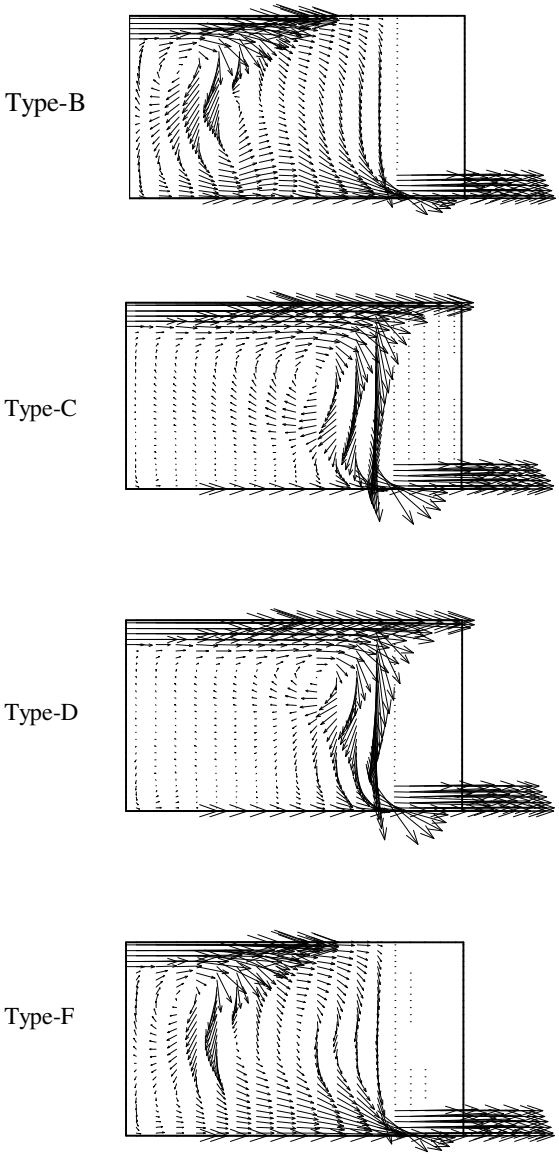

Fig. 4. The effect of magnetic field configurations on flow pattern (B = 1 Tesla).

This can also be concluded from figure 5 in which the variations of normal velocity at the exit is drawn along the width of the strip.

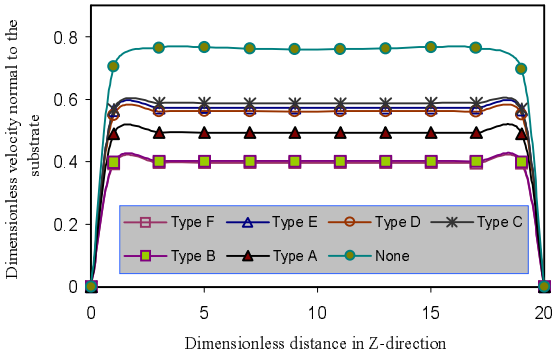

Fig. 5. Variations of normal velocity at the exit along the z-direction for different magnetic configurations (b=1 Tesla).

The dissipation of liquid steel superheat at the chilled substrate was studied in this model. It can be deduced from the temperature distribution within the reservoir that the flow pattern considerably affects the dissipation rate of superheat as expected. In order to evaluate the effect of magnetic flow modifier on the rate of heat dissipation, a *Nu* number was defined as $Nu = \frac{\bar{h}d}{k}$ where $\bar{h}$ (heat transfer coefficient) was calculated from heat flux to the chilled belt and the temperature difference between substrate and inlet liquid steel. Figure 6 shows the variations of *Nu* along the chilled belt under different magnetic configurations. As can be seen from this figure the most uniformity of *Nu* along the substrate was obtained using the type-F. Nevertheless the highest dissipation rate was achieved for type-B.

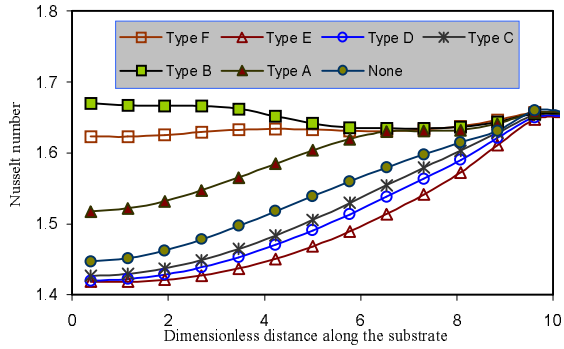

Fig. 6. Variations of Nu along the chilled belt for different magnetic configurations (B=1 Tesla).

5.Conclusions

From predicted results of the present model it can be concluded that the magnetic flow control device can be successfully applied to metal delivery of single-belt caster. It was found that the DC magnetic field shifts the recirculation zone towards the back wall of the reservoir and lower the impinging intensity over the chilled substrate. It was recognized that the combination of vertical and horizontal types of magnetic devices results in a better response for flow

modification. Furthermore, the latter type leads to the most uniformity in the dissipation rate of the superheat in the reservoir among the examined configurations.

Acknowledgement
The authors are very grateful to Iran University of Science and Technology for its financial support.

REFERENCES

[1] R.I.L. Guthrie and Mihaiela Isac , *Steel Research*, Vol. 70, Jan. 1999, p. 343.
[2] K.H. Spitzer and K. Schwerdtfeger, *Iron & Steelmaker* ,22(1997), p.47.
[3] Klaus Schwerdtfeger, K.H. Spitzer, J. Kroos, P. Funke and K.H. Hower, *ISIJ International*, Vol. 40 (2000), No.8, p.756
[4] Pedro G. Q. Netto and R.I.L. Guthrie, *ISIJ International* , Vol. 40(2000),No.5, p. 460.
[5] Carol Jefferis,PhD. Thesis , Department of Mining and Metallurgical Engg., McGill University, 1996
[6] Tian C, Mazumdar D & R.I.L. Guthrie, *Metallurgical and Materials Transaction B*, Vol. 30, Jan. 1999, p.891.
[7] Guthrie R.I.L. & M. Isac, Recent Research Developments in Met. & Science, Vol. 2, Jan. 1999, p. 25.
[8] B.E. Launder and B.I. Sharma, , *Letters In Heat and Mass Transfer*, Vol. 1, p. 131 (1974).
[9] K.Y.M. Lai, M. Salcudean, S. Tanaka and R.I.L. Guthrie, Mathematical modelling of flows in large tundish systems in steelmaking, *Metall. Trans.,* Vol. 17B, p. 449 (1986).
[10] S.V. Patankar, *Numerical Heat Transfer and Fluid Flow*, Hemisphere, Washington, D.C., (1980).
[11] S.H. Seyedein and M. Hasan, A 3-D numerical prediction of turbulent flow, heat transfer and solidification in a continuous slab caster for steel, *Canadian Metallurgical Quarterly*, vol. 37: (3-4), p. 213 (1998).